

# An Investigation on Hybrid Composite Drive Shaft for Automotive Industry

Gizem Arslan Özgen, Kutay Yüçetürk, Metin Tanoğlu, Engin Aktaş

**Abstract**—Power transmitted from the engine to the final drive where useful work is applied through a system consisting of a gearbox, clutch, drive shaft and a differential in the rear-wheel-drive automobiles. It is well-known that the steel drive shaft is usually manufactured in two pieces to increase the fundamental bending natural frequency to ensure safe operation conditions. In this work, hybrid one-piece propeller shafts composed of carbon/epoxy and glass/epoxy composites have been designed for a rear wheel drive automobile satisfying three design specifications, such as static torque transmission capability, torsional buckling and the fundamental natural bending frequency. Hybridization of carbon and glass fibers is being studied to optimize the cost/performance requirements. Composites shaft materials with various fiber orientation angles and stacking sequences are being fabricated and analyzed using finite element analysis (FEA).

**Keywords**—Composite propeller shaft, hybridization, epoxy matrix, static torque transmission capability, torsional buckling strength, fundamental natural bending frequency.

## I. INTRODUCTION

SHAFTS are used to transmit the rotary load from one component to another. Metallic drive shafts have limitations of weight, low critical speed and vibration characteristics. Besides, steel drive shafts are manufactured in two pieces to increase the fundamental natural frequency. Numerous solutions, such as flywheels, harmonic dampers, vibration shock absorbers, multiple shafts with bearings and couplings, and heavy associated hardware, have shown limited success in overcoming the problems [1].

In the automotive industry, many of the problems caused by traditional metal cardan shafts can be solved using composite cardan shafts. The composites enable the replacement of the two-piece metal shaft with a single component composite shaft due to their higher specific elastic modulus.

This study provides a groundwork to develop hybridized hollow shaft. The term hybrid shafts referred to fabrication technique using multiple types of reinforcement layers. Using hybrid fiber system in composite shafts further enhances the property tailoring ability. Especially for the structures under varied stresses such as composite shafts, sensitive property tailoring may provide some cost advantages. Carbon fiber drive shafts achieve torsional performance but due to the cost constraint, a hybrid of layers of carbon-epoxy and E-glass-

epoxy was introduced. Required bending natural frequencies and torque capacities can also be satisfied without any problem. Researchers studied on hybrid shafts using multiple types of reinforcement layers. Some of the studies focus on the torsional performance of carbon and glass reinforced hybrid composite shafts that were manufactured by filament winding technique [2], [7]. Others [8], [10] considered aluminum/glass composite shafts.

Badie et al. [2] also examined stacking sequence and orientation angles effects on torsional stiffness of hybrid glass/carbon fiber shafts. The numerical results were validated by results obtained from analytical solutions. As a result of this study, they determined that an orientation angle of 45° is best in order to achieve the maximum stiffness.

In another research, Abu Talib et al. [3] investigated on stacking sequence effects with a combination of glass and carbon fibers. In this study, they developed carbon and glass fibers within an epoxy matrix from four layers stacked as 45°glass/45°glass/0°carbon/90°glass. A FEA was used to design carbon and glass fiber epoxy matrix composite shafts. The results of the study revealed that worst stacking sequence results in 46.07% less strength than a shaft with best stacking sequence. When the winding angle was changed from 0° to 90°, natural frequency of the shaft was decreased 44.5%.

Sevkat et al. [4] studied on the effect of torsional strain-rate and lay-up sequences of fibers on the performance of hybrid composite shafts by using numerical and experimental approach. In this study, glass and carbon fiber reinforced hybrid shafts with three lay-up sequences were manufactured using filament winding technique. The composite shafts manufactured with same geometry, same amount of glass and carbon reinforcement and same amount of matrix material. As a result of this study, the change in lay-up sequence of hybrid layers significantly affects the torsional performance of the shafts. Usage of glass in outer layers increases the maximum twisting angle and provides some ductility to composite shafts. Hence carbon increases the torque resistance but decreases the ductility of composite shafts. By altering glass and carbon stacking sequences, desired twisting angle and torque resistance can be achieved.

Rastogi [5] analyzed and designed hybrid composite shaft of carbon/epoxy and glass/epoxy to optimize the cost versus performance requirements. Experimentally, composite tubes of

Gizem Arslan Özgen is with the Tirsan Kardan Research and Development Center, Manisa, and with the Izmir Institute of Technology, Department of Mechanical Engineering, Urla, Izmir, Turkey (e-mail: g.arslan@tirsankardan.com.tr).

Kutay Yüçetürk and Engin Aktaş are with the <sup>3</sup>Izmir Institute of Technology, Department of Civil Engineering, Izmir, Urla, Turkey (e-mail: enginaktas@iyte.edu.tr, kutayyuceturek@iyte.edu.tr).

Metin Tanoğlu is with the Izmir Institute of Technology, Department of Mechanical Engineering, Izmir, Urla, Turkey (e-mail: metintanoglu@iyte.edu.tr).

fiber orientation angles of  $\pm 45^\circ$  experience higher load carrying capacity and higher torsional stiffness. The natural frequency increases with decreasing fiber orientation angles as a result of FEA. The results from the numerical results obtained from the FEA were used to validate the analytical solutions. The effect of stacking sequence on the buckling strength is observed. It is concluded that the best stacking sequence is [45/45/0/90] and the worst is [0/90/45/45] between trials.

Tariqa et al. [6] investigated the effects of hybrid fiber reinforcements including carbon-glass and carbon-aramid on the performance of hollow shafts. As a result of this research, the researchers had an explanation on hybridization of shafts as compared to carbon fiber shafts. It is concluded that torsional properties decrease as carbon fiber shafts are hybridized with glass or aramid fibers. However, hybrid shafts can be employed in applications where a tradeoff is required between two or more properties. Glass fibers are much less costly than carbon fiber and hence carbon-glass hybrid shafts provide a relatively better performance while being cost effective. Similarly, carbon-aramid hybrid shafts show low weight than pure carbon fiber shafts hence this carbon-aramid shafts can be used when weight and torsional strength are required for an application. Moreover, glass and aramid fibers are known for their low cost and high flame resistance respectively and hence a hybrid fiber with carbon fiber not only provides strength but also add up other advantages. Hybrid reinforced shafts are more resistant to mechanical wear as compared to pure carbon fiber shafts.

A composite drive shaft design example, presented by Swanson [7], used a composite shaft that has 1730 mm length and a 50.8 mm average radius for the analyzes. The hybrid composite tube consists of three layers: ( $\pm 45^\circ$ ,  $90^\circ$ ) glass-epoxy and  $0^\circ$  carbon-epoxy layer. The ultimate torque was 2030 Nm and the minimum natural frequency in bending is 90 Hz.

Lee et al. [8] developed a shaft in which a combination of composite and metallic part was utilized. The results of the study revealed that a hybrid shaft offers 75% mass reduction and 160% increase in torsional strength compared to the full metallic shaft. Mutasher [9] also examined the hybrid aluminum/composite shaft with the prediction of torsional strength using analytical techniques. The study inferred that an increase in a few composite layers leads to an increase in torsional strength with a compromise on weight. Mutasher investigated the torsional behavior of hybrid shafts using FE analysis. For the hybrid shaft that has aluminum tube inside and six layers of carbon fiber/epoxy outside, the maximum torque was 295 Nm.

Kim [10] manufactured hybrid shaft which had stainless steel surface and composite core. Carbon/epoxy layers were laid in to the steel tubing. They found that hybrid shaft had less tilting angle and higher natural frequency compared to that of non-hybrid steel shaft.

## II. DESIGN AND ANALYSIS

The study is based on the FEA and validation of model with the experiments. Prior to full scale shaft tests, lamina coupons are tested to obtain homogenous lamina properties to be used in FE model.

### A. Analytical Calculations

Analytical expressions to obtain the bending natural frequency, critical buckling torque and maximum torsional strength are available in the literature [11], [12]. They are used prior to experiments, to have a measure of magnitudes to check FEM. These expressions are briefly presented below for reference. The bending natural frequency for free-free ends is defined as in [11]:

$$f_n = \frac{22.4}{2\pi} * \sqrt{E_{eff} * \frac{I}{mL^4}} \quad (1)$$

where m: Mass per unit length;  $E_{eff}$ : Effective modulus in x direction; I: Moment of inertia around the orthogonal axis to x; L: Length of the shaft.

Effective modulus in x,  $E_{xeff}$  and in hoop direction,  $E_{heff}$  are determined as [12]:

Given that Tr is the transformation matrix;

$$[\bar{Q}] = [Tr(\theta)]^{-1} [Q] * [Tr(\theta)]^{-T} \quad (2)$$

$$A_{ij} = \sum_{k=1}^n [\bar{Q}_{i,j}]_k \quad (3)$$

$$E_{xeff} = [A_{11} - A_{12}^2/A_{22}] * 1/t \quad (4)$$

$$E_{heff} = [A_{22} - A_{12}^2/A_{11}] * 1/t \quad (5)$$

where t: total thickness; A: In plane stiffness matrix; Q: Reduced stiffness matrix.

$$Q_{11} = \frac{E_1}{1 - \nu_{12}^2 * \frac{E_2}{E_1}} \quad Q_{22} = \frac{E_2}{1 - \nu_{12}^2 * \frac{E_2}{E_1}} \quad (6)$$

$$Q_{12} = Q_{21} = \frac{E_2 * \nu_{12}}{1 - \nu_{12}^2 * \frac{E_2}{E_1}} \quad Q_{66} = G_{12}$$

Another important parameter that needs to be checked is the buckling torque, which is critical when the wall of the shaft is getting thinner relative to the radius. Critical buckling torque,  $T_{cr}$  is highly affected by the hoop resistance as it can be seen in [13]

$$T_{cr} = (2\pi r_m^2 t)(0.272) * (E_{xeff} E_{heff}^3)^{0.25} * \left(\frac{t}{r_m}\right)^{1.5} \quad (7)$$

Finally, the maximum torque ( $T_{max}$ ) capacity that the drive shaft can transfer is simply related to the shear strength and the geometry of the shaft.

$$T_{max} = \tau_{12} * \frac{J}{r_o} \quad (8)$$

where  $r_m$ : mean radius; J: Polar moment of area;  $\tau_{12}$ : Shear strength of the composite;  $r_o$ : outer radius of the shaft.

### B. Finite Element Model

Finite element model is created to be able to predict the behavior of the composite shafts. At the current stage, stacking

angles are fixed to  $55^\circ$ . The main goal behind creating simple configuration is to calibrate and validate the modelling technique, winding and testing processes. ANSYS Software v17.2 is used with ACP Pre-Post module. The mesh element is SOLSH190 which is an 8 node 3-D element specially developed for thin to moderately thick shell members [14,15].

In the ACP model of ANSYS, the plies added starting from a constant mandrel diameter ( $d=70\text{mm}$ ) and stacked in outward normal direction. Every ply is defined individually and this structure is converted into solid model by the software for the analysis. This way of modelling enables the ply-wise examination of the failure and behavior.

The stacking sequences for each specimen is provided in TABLE I. The sequence is provided from outer layer to inner layer.

TABLE I  
STACKING SEQUENCES OF SPECIMENS

Specimen ID	Stacking (inward)	$D_{in}   D_{out}$ (mm)
82.1Cb15(55)	$C[\pm 55]_{15}$	70   82
82.6GI10(55)	$G[\pm 55]_{10}$	70   82.6
80.2Cb6GI6(55)	$C[\pm 55]_6 + G[\pm 55]_6$ $t_c=2.75 + t_g=2.55$	70   80.2
82.8GI6Cb6(55)	$G[\pm 55]_6 + C[\pm 55]_6$ $t_g=3.3 + t_c=3.1$	70   82.8
81.2GI4Cb8(55)	$G[\pm 55]_4 + C[\pm 55]_8$ $t_g=2.2 + t_c=3.4$	70   81.2
80Cb8GI4(55)	$C[\pm 55]_8 + G[\pm 55]_4$ $t_c=3.35 + t_g=1.65$	70   80

### 1) Lamina Properties

Lamina properties are defined within ACP-Pre module. ACP-Pre module imports the shell geometry adds the ply, one on each other in the preferred direction. Polar properties of a single layer of glass (+55° stack) and carbon composite are provided in Fig. 1 and Fig. 2.

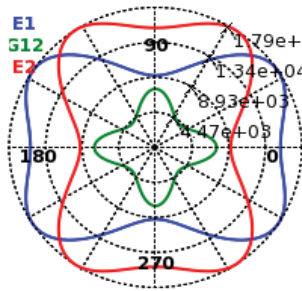


Fig. 1 Glass lamina single layer polar properties (+55)

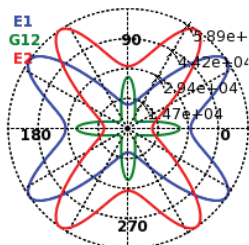


Fig. 2 Carbon lamina single layer polar properties (+55)

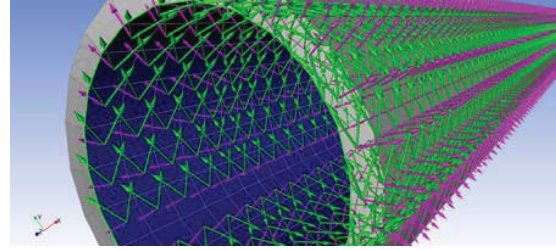


Fig. 3 Fiber direction and plying orientation

### 2) Modal Analysis

Modal behavior of the shaft is important for its applicability in vehicles since the operational frequency must not coincide with the natural frequencies of the shaft. Moreover, modal analysis results may provide useful information on the validation of the numerical model.

The parameters of the winding method coupons are used for the analysis which is presented in latter section. Free boundary condition is defined for the modal analysis. Thus the first 6 modes are omitted which resulted 0 Hz due to rigid body motion. Shaft is meshed with max member size of 45mm. Results of the analysis are provided in Table II.

TABLE II  
FEM MODAL ANALYSIS RESULT OF SPECIMENS

Specimen ID	1 <sup>st</sup>   2 <sup>nd</sup> Mode (Hz)
82.1Cb15(55)	124   340
82.6GI10(55)	102   274
80.2Cb6GI6(55)	121   328
82.8GI6Cb6(55)	102   274
81.2GI4Cb8(55)	118   320
80Cb8GI4(55)	120   323

### 3) Strength Analysis

Torsional capacity of the shaft is the first property to be checked for the applicability of a design. The shaft should be capable of transferring the torsional force from one end to the other end. In application, the two ends of the shaft shall be attached to the transmission system with insert type joints. To represent the presence of inserts, moment forces are applied from inner surface through 10cm length (see Fig. 5). If the torsion is applied from the edge line of the tube, there were anomalies in the stress distribution due to concentrated application of the load. No other boundary condition is required to be defined for torsional capacity analysis.

Once the geometry and stacking sequence defined in the model, torsional capacity is found by changing the applied moments until one of the failure limits violated. At this stage of project, all available built-in failure criteria are checked. For the absent material properties that are needed to check some of the failure criteria, default limits of "Epoxy E-Glass Wet" and "Epoxy Carbon UD 230GPa Wet" are used which are predefined in ANSYS v17.2. TABLE lists the criteria that are used for the failure state. TABLE IV summarizes the resultant torsional capacity of the shafts.

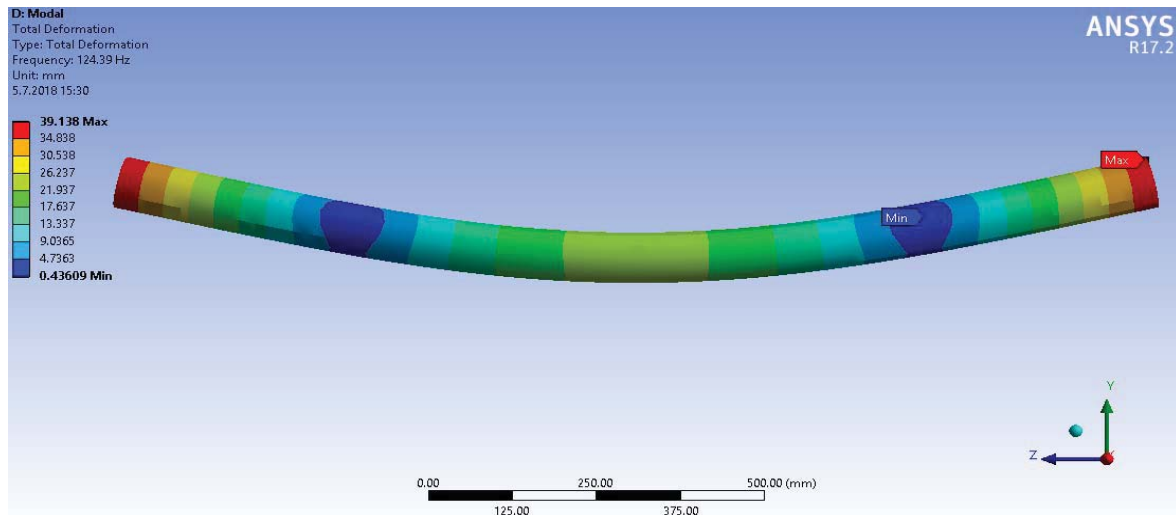


Fig. 4 Typical 1st Mode Shape of the Shaft

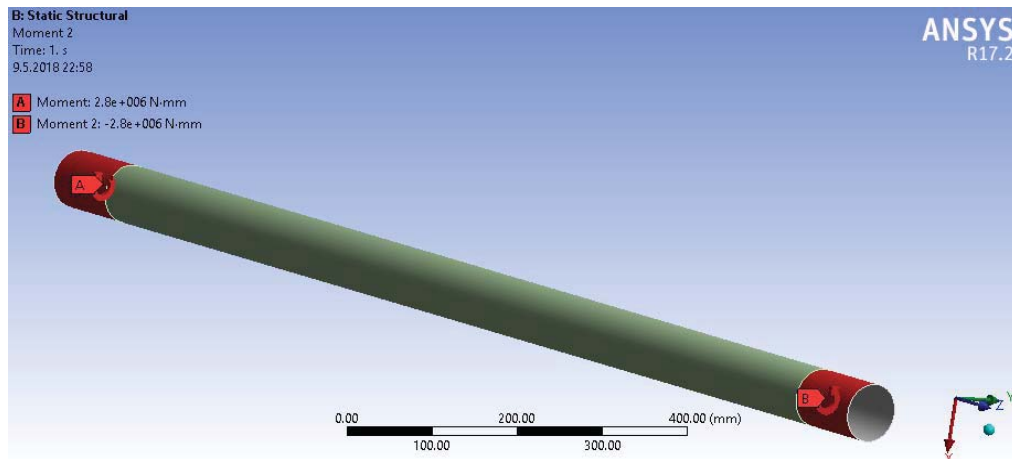


Fig. 5 Moment application at both ends through insert contact surfaces

TABLE III  
FAILURE LIMITS FOR THE TORSIONAL CAPACITY ANALYSIS

	Failure Type
Max Strain	Fiber Failure
	Matrix Failure
	In-Plane Shear Failure
Max Stress	Fiber Failure
	Matrix Failure
	In-Plane Shear Failure
Tsai-Wu	Tsai-Wu
Tsai-Hill	Tsai-Hill
Hoffman	Hoffman
Hashin	Fiber Failure
	Matrix Failure
	Fiber Failure
Puck	Matrix Tension /Compression Failure
	Matrix Shear Failure

#### 4) Torsional Buckling Analysis

Torsional buckling analysis is performed with Eigenvalue buckling module of the Ansys. The results are obtained as load factor in software and converted to buckling torque by simply

multiplying with the applied moment. One end of the tube is fixed to avoid translational modes and obtain the correct load factor directly.

The results of the torsional buckling analysis are provided in TABLE IV for all specimens. It is observed that the critical buckling torque increases with increasing carbon composite content and thickness of the tube. However, when the inner surface of the shaft (load application layer) is glass the critical buckling torques are relatively diminishes in numerical results.

TABLE IV  
FEM RESULTS FOR THE TORSIONAL CAPACITY AND CRITICAL BUCKLING TORQUE OF THE SPECIMENS

Specimen ID	FEM Torque Capacity (Nm)	FEM Critical Buckling Torque (Nm)
82.1Cb15(55)	2600	28600
82.6GI10(55)	1440	16450
80.2Cb6GI6(55)	2000	19000
82.8GI6Cb6(55)	3000	23500
81.2GI4Cb8(55)	2880	18000
80Cb8GI4(55)	1640	15260



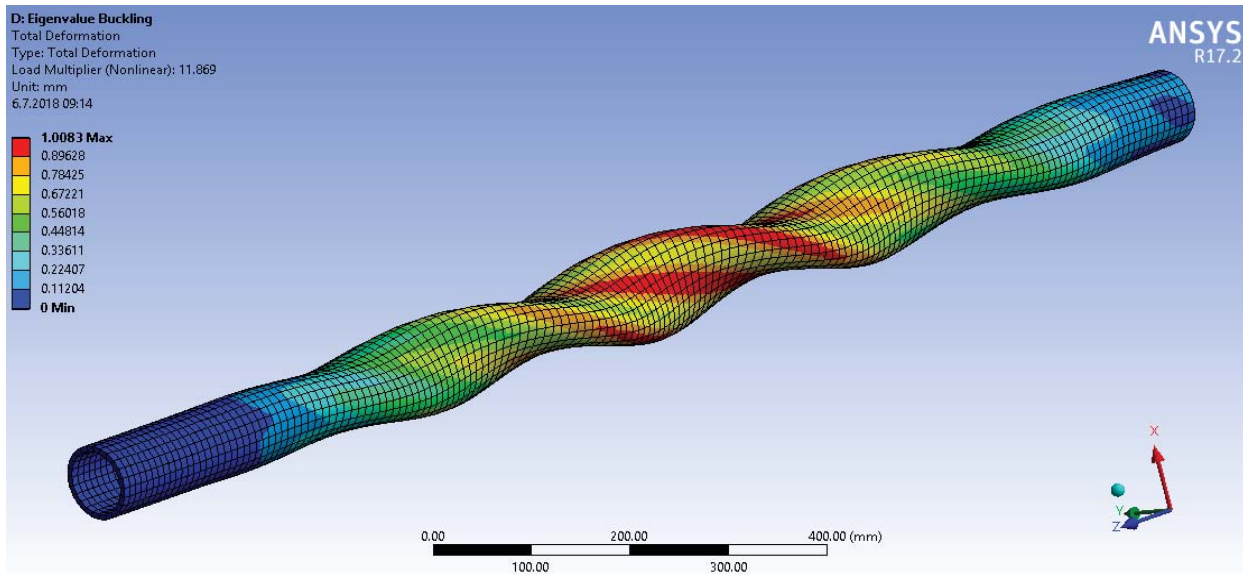


Fig. 6 Torsional Buckling Analysis typical torsional buckling mode

### C. Manufacturing Technique

The filament winding method is used because of the tube geometry. Winding process is done fully automatic with a CNC controlled winding machine. The system controls the back and forth movements, ensures constant tension on fibers and the precision of the winding process.

The specimens with different mechanical properties are obtained by continuous winding of fibers in different angles and/or with different sequence. After the wrapping process is finished, a plastic film that does not stick to the piece is wrapped on the piece. This allows the part to be compressed and the film is removed after the curing process is finished. After winding, the mandrel is placed in a furnace. The thermoset resin material, which is heated to provide a specific heating profile, cures and hardens after a while. The mandrel is then removed.



Fig. 7 Filament winding equipment

### D. Design and Results of Experiments

#### 1) Coupon Tests

Firstly, to create the finite element model of the shaft and make use of analytical expressions, homogenous material properties are determined through coupon testing. Coupons are created by two manufacturing techniques which are vacuum

infusion and winding on flat plate. Significant difference in elastic modulus is observed between two production methods. As it is mentioned in latter section, the winding produced coupon results showed better approximation to the shaft modal experiment results when employed in FE model of the shaft. The difference is significant particularly for the E-glass epoxy as it can be seen in Tables VI and VII.

TABLE V  
FIBER AND MATRIX PROPERTIES

	Tensile Strength (MPa)	Tensile Modulus (GPa)	Strain (%)	Density (g/cm <sup>3</sup> )
Glass Fiber Şişecam FWR6 12 K	2400	73	1.5	2.6
Carbon Fiber Aksa A 49 12K	4900	250	2	1.79
Epoxy Resin Hunstman MY740	61	3.6	2	1.16

TABLE VI  
E-GLASS EPOXY COUPON TEST RESULTS (VACUUM INFUSION VS WINDING)

	θ	Vacuum Infusion	Winding
Tensile Strength (MPa)	0°	649.7 (±) 97.5	610.0 (±) 25.4
	90°	25.7 (±) 2.2	14.1 (±) 1.7
Elastic Modulus (GPa)	0°	39.7 (±) 3.6	27.9 (±) 2.6
	90°	11.5 (±) 0.9	7.3 (±) 1.5
Density:		1.56 g/cm <sup>3</sup>	
ν:		0.287	

TABLE VII  
CARBON EPOXY COUPON TEST RESULTS (VACUUM INFUSION VS WINDING)

	θ	Vacuum Infusion	Winding
Tensile Strength (MPa)	0°	1250*	1081.7 (±) 31.1
	90°	20.3 (±) 1.9	15.2 (±) 6.3
Elastic Modulus (GPa)	0°	110*	108.3 (±) 0.9
	90°	9.6 (±) 1.1	8.8 (±) 1.1
Density:		1.2 g/cm <sup>3</sup>	
ν:		0.33	

\*St. Dev. is not available

## 2) Impact Hammer Test of the Shaft

Impact hammer test is conducted on each of the shafts. The shaft is supported at four points with low stiffness supports. 3 piezoelectric accelerometers are attached on the shaft and impact is given by impact hammer. There are no additional boundary conditions. Tests are conducted in the R&D labs of Tirsan Company. Test results are given in

TABLE VIII for the 6 shafts.

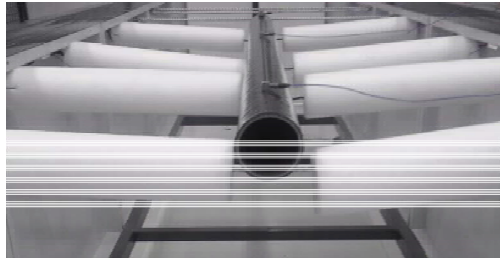


Fig. 8 Impact Hammer Test Apparatus

TABLE VIII  
GEOMETRIC PROPERTIES OF SHAFT SPECIMENS AND IMPACT HAMMER TEST RESULTS {C: CARBON EPOXY G: GLASS EPOXY}

Specimen ID	1 <sup>st</sup>   2 <sup>nd</sup> Mode (Hz)
82.1Cb15(55)	110   305
82.6GI10(55)	100   270
80.2Cb6GI6(55)	110   296
82.8GI6Cb6(55)	105   282
81.2GI4Cb8(55)	102   280
80Cb8GI4(55)	108   292

t= thickness in mm for carbon or glass, D= Inner or outer diameter of the specimen.

## III. RESULTS AND DISCUSSION

This project deals with the design, material selection, modelling, optimization of stacking sequence, fabrication and performance testing of composite drive shaft for a small vehicle. But current study aims to reveal the suitability of fiber composites in the drive shaft industry and predictability of mode frequencies of shafts which is a must requirement for the drive shaft applications. Shafts that are made of Carbon/epoxy, E-glass/epoxy and hybrid of these composites are modeled, manufactured and tested for the natural mode frequencies. The FE models were tried to be validated by looking at the first natural mode frequency. The findings are tabulated in Table IX. The results match with the maximum error of 14%. Error is calculated by;

$$\%Error = \frac{f_{FEM} - f_{EXP}}{f_{EXP}} * 100 \quad (1)$$

Some final comments are;

- If the manufacturing method is winding, the material lamina mechanical properties should be obtained through the winded specimens. Otherwise, the modulus and the strength values may be unrepresentative of the production due to different volume fraction of the composite media.
- Inner most layer is the most critical layer for the torsional strength analysis, because all the force is applied on it and

need to be transferred through laminate surface to outer ply layers

- Critical buckling torques were clearly much higher than the target design torque
- Torsional tests on the specimens would reveal the performance of the FEM and strength analysis at the next phase of this project

TABLE IX  
1ST AND 2ND NATURAL MODE FREQUENCY COMPARISON OF EXPERIMENTAL AND FEM RESULTS

Specimen ID	FEM 1 <sup>st</sup>   2 <sup>nd</sup> Mode (Hz)	Experimental 1 <sup>st</sup>   2 <sup>nd</sup> Mode (Hz)	Error (%) 1 <sup>st</sup>   2 <sup>nd</sup> Mode
82.1Cb15(55)	124   340	110   305	+13   +12
82.6GI10(55)	102   274	100   270	+2   +2
80.2Cb6GI6(55)	121   328	110   296	+10   +11
82.8GI6Cb6(55)	115   313	105   282	+10   +11
81.2GI4Cb8(55)	118   320	102   280	+14   +13
80Cb8GI4(55)	120   323	108   292	+12   +11

## ACKNOWLEDGMENT

We would like to thank the Tirsan R & D Center, which enabled and supported us during the realization of this work.

## REFERENCES

- [1] Troung L, Leslie JC, Blank B, Frick G. Composite drive shafts: technology and experience. SAE Special Publications 1996:43–59.
- [2] Badie MA, Mahdi E, Hamouda AMS. An investigation into hybrid carbon/glass fiber reinforced epoxy composite automotive drive shaft. Mater Des 2011;32: 1485–500.
- [3] Abu Talib AR, Ali A, Badie MA, Lah NA, Golestaneh AF. Developing a hybrid, carbon/glass fiber-reinforced, epoxy composite automotive drive shaft. Mater Des 2010;31(1):514–21.
- [4] Sevkati E, Tumer H, Halidun Kelestemur M, Dogan S. Effect of torsional strain-rate and lay-up sequences on the performance of hybrid composite shafts. Mater Des 2014; 60:310–9.
- [5] Rastogi N. Design of composite driveshafts for automotive applications. SAE, technical paper series, 2004-01-0485; 2004.
- [6] Mateen Tariqa M, Nisara S, Shaha A, Akbar S, Khanc M. A, Khand S. Effect of hybrid reinforcement on the performance of filament wound hollow shaft. Compos Struct 2018; 184: 378–387
- [7] Swanson SR. Introduction to design and analysis with advanced composite material. Upper Saddle River (New Jersey): Prentice Hall; 1997.
- [8] Lee DG, Kim JW, Hwang HY. Torsional fatigue characteristics of aluminum composite co-cured shafts with axial compressive preload. J Compos Mater 2004;38: 737–56.
- [9] Mutasher SA. Prediction of the torsional strength of the hybrid aluminum/composite drive shaft. Mater Des 2009;30(2):215–20.
- [10] Kim HS, Kim BC, Lim TS, Lee DG. Foreign objects impact damage characteristics of aluminum/composite hybrid drive shaft. Compos Struct 2004;66(1– 4):377–89.
- [11] Kaw, Autar K. Mechanics of Composite Materials. Boca Raton: CRC Press, 2006.
- [12] Barbero, Ever J. Introduction to Composite Materials Design. Boca Raton: CRC Press, 2018.
- [13] Bert CW, Kim CD. Analysis of buckling hollow laminated composite drive shafts. Compos Sci Technol 1995; 53:343–51.
- [14] ANSYS, Inc. SHARCHNET. SHARCHNET Web Site. (Online) [https://www.sharcnet.ca/Software/Ansys/16.2.3/en-us/help/ans\\_elem](https://www.sharcnet.ca/Software/Ansys/16.2.3/en-us/help/ans_elem).
- [15] ANSYS Workbench User's Guide, Canonsburg: ANSYS, Inc., 2016.